DEFORMATION AND FAILURE MECHANISMS IN A SPRAY FORMED Al ALLOY-SiC COMPOSITE

J. LLORCA, J. RUIZ and M. ELICES

Department of Materials Science, Polytechnic University of Madrid
Ciudad Universitaria, 28040-Madrid, Spain

ABSTRACT

In a study of the deformation and failure mechanisms in a spray formed 2618 Al alloy reinforced with 15% vol. SiC particulates, it was found that this processing route gives composites with excellent tensile and fracture properties, with the exception of the tensile ductility in the peak-aged condition. Failure is, then, precipitated by the early fracture of coarse SiC particulates during deformation. Improvement of the tensile ductility, while maintaining the fracture toughness, requires a reduction of the particulate size and also of matrix inclusion content.

KEYWORDS

Metal-matrix composites; particulate fracture; ductility.

INTRODUCTION

The mechanical properties of discontinuously reinforced Al-based composites have been object of increasing attention in recent years. The primary goal was to improve the tensile ductility and fracture toughness in order to meet the requirements of the aerospace and automotive industries, and new manufacturing methods have been introduced to achieve the desired properties. Most of the research was carried out on composites produced by various casting procedures (Nakagawa and Gungor, 1990; Kamat *et al.*, 1989; Lloyd, 1991) or hot pressed by powder metallurgy techniques (McDanels, 1985; Lewandowski *et al.*, 1989; Arsenault *et al.*, 1991), but very little information is available about composites manufactured by other routes.

Spray forming offers an appealing alternative to hot isostatic pressing to produce high performance particulate-reinforced metal-matrix composites (MMC) at lower cost. The advantages of this technique include reduced segregation levels, tolerance of tramp impurities and ready incorporation of ceramic particulates. The production of an ingot by spray deposition can be accomplished by introducing the ceramic particulates into the standard spray deposition metal procedure, leading to co-deposition with the atomised metal onto the substrate. If the conditions of atomising and particulate feeding are carefully controlled, a very uniform distribution of the particulates within the matrix is obtained and the matrix density is between 95 to 98% of the theoretical one (Willis, 1988).

The mechanisms of deformation and failure at ambient temperature in a spray formed Al alloy-SiC particulates composite are studied here. The experimental determination of the mechanical properties is completed with an analysis of the fracture processes by optical and scanning electron microscopy, and with the numerical simulation of the evolution of stresses and strains in the matrix and in the reinforcement during composite deformation. The results provide valuable information which may be used to improve

the fracture toughness and tensile ductility of spray formed composites by changing the matrix chemical composition and the particulate size.

MATERIALS AND EXPERIMENTAL PROCEDURES

A spray formed 2618 Al alloy reinforced with 15 vol. % of coarse SiC particulates ($\approx$ 16 μm in diameter) was used in this investigation. The material was supplied by Cospray (Alcan Int. Ltd.) in the form of extruded rectangular bars (cross section 25.4 mm x 62.5 mm). After extrusion, the bars were solution heat treated at 530^{0}C for 1 hour, water quenched, and cold stretched up to 2% to relieve the residual stresses introduced by quenching. Afterwards, they were artificially aged at 190^{0}C for 10 hours to reach the peak-aged condition (T651), and tensile and fracture toughness specimens were machined from the bars. Several specimens were then solution heat treated (1 hour at 530^{0}C) to eliminate the effect of the prior thermo-mechanical treatments, and naturally aged at room temperature (T4). The unreinforced 2618 Al alloy also supplied by the manufacturer, processed by the same route, was subjected to the same thermo-mechanical treatment. The only difference between the composite and the control alloy heat treatments was the aging time, which was increased to 24 hours in the unreinforced material considering the faster precipation kinetics in the former (Suresh *et al.*, 1989).

For each material and heat treatment two tensile tests were carried out in accordance with ASTM Standard E8M. The average strain rate employed was 10^{-4} sec^{-1}. In addition, two more tensile tests were performed on the composite material in the T4 and T651 conditions. The specimens were periodically unloaded during these tests to study the evolution of the Young's modulus during composite deformation. Duplicated fracture toughness tests were carried out on compact tension specimens in the peak-aged condition of the composite and unreinforced alloy. Specimen thickness was 25.4 mm, the crack being oriented in the L-T direction.

The fracture surfaces were examined by scanning electron microscopy to ascertain the main failure mechanisms for each material and heat treatment. The chemical composition of the inclusions was determined by energy dispersive X-ray microanalysis. The specimens periodically unloaded during the tensile tests were sliced through the center in the loading direction with a low speed diamond wheel, using oil as a lubricant, and metallographically polished. The polished surfaces were examined under optical and scanning electron microscopes to study the failure mechanisms at a distance from the fracture surfaces.

RESULTS

Tensile and fracture toughness properties of the materials tested are shown in Table 1 (each value is the average of two tests). The addition of the SiC particulates increases

Table 1. Ambient temperature mechanical properties

Material	E (GPa)	σ_y (MPa)	σ_u (MPa)	ϵ_u (%)	K_{Ic} (MPam$^{1/2}$)
2618 (T4)	70	222	470	16.4	—
2618 (T651)	70	418	445	7.2	22.7
2618+SiC (T4)	94	254	482	12.3	—
2618+SiC (T651)	95	484	503	4.1	21.3

the stiffness considerably (around 35%) and there are also improvements in the yield strength, σ_y, and the failure strength, σ_u, as compared with the unreinforced alloys in both the underaged and the peak-aged conditions. The fracture toughness is only slightly affected by the ceramic reinforcement, and the value measured for the peak-aged composite is very good. Two recent articles on fracture properties of particulate

and whisker-reinforced MMCs (Goolsby and Austin, 1989; Roebuck and Lord, 1990) indicated that the valid K_{Ic} values of MMCs with yield strengths in the range 350-500 MPa fall within a relatively narrow toughness range of 13-17 MPa m$^{1/2}$, regardless of the matrix composition and volume fraction of reinforcement.

The main limitation of this spray formed composite is the low ductility of the peak-aged material, and subsequent studies were carried out to elucidate the causes of this behaviour. The evolution of the composite Young's modulus, E_c, with the applied strain and stress is shown in Figs. 1a and 1b for the underaged and peak-aged conditions respectively. The results plotted in Fig. 1a show that the damage (reflected in the reduction in E_c) develops very early but that the damage rate is higher in the peak-aged composite. However, if the modulus is plotted *vs* the stress, both materials exhibit very similar behaviour up to 400 MPa, and beyond that point the underaged composite shows a faster drop in its elastic properties.

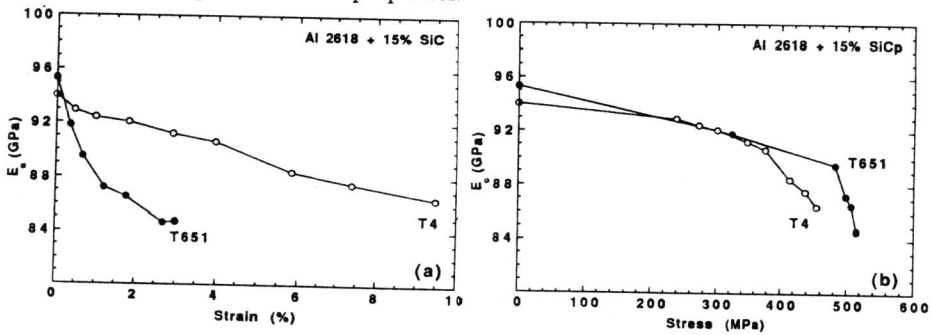

Fig. 1. Evolution of the composite Young's modulus with (a) strain (b) stress.

The fractographic analysis of the fracture surfaces shows that the unreinforced alloy failed by the mechanism of nucleation, growth and coalescence of voids around intermetallic inclusions (Fig. 2). Energy dispersive X-ray microanalysis indicated that these inclusions were made up of Al, Ni and Fe, the two latter having been added to the alloy to enhance the microstructural stability under thermal exposure. The inclusions were distributed within the Al alloy grains, at the grain boundaries and at the particulate-matrix interfaces, and the average size was $\approx$ 4 μm, with an equiaxed shape. More detailed analyses by X-ray diffraction confirmed that the inclusions were monoclinic Al_9NiFe (Zhang and Derby, 1991).

Microscopically, the composite fracture surfaces exhibit a ductile appearance (Fig. 3). SiC particulates, with an average size equal to or larger than 10 μm, are present in the fracture surfaces in both T4 (Fig. 3a) and T651 (Fig. 3b) conditions, although the number of particulates is larger in the latter. Smaller voids, around the intermetallic inclusions, are also seen, specially in the T4 temper. The matrix is heavily deformed around the particulates and well bonded to them, as can be observed at higher magnification (Fig. 3c), and interfacial debonding does not seem to play an important role in the composite failure. Most of the SiC particulates show a clean fracture, although some of them exhibit markings (see arrow in Fig. 3c). These appear to be Wallner lines, and were already reported in SiC particulates fractured within an Al matrix (Healy and Beevers, 1991).

The polished surfaces of the samples sliced through the middle provided more information about the particulate fracture. Broken particulates were observed throughout the gauge length and not only near the fracture surfaces for both heat treatments. The broken particulates can be separated into two groups: large equiaxed particulates with

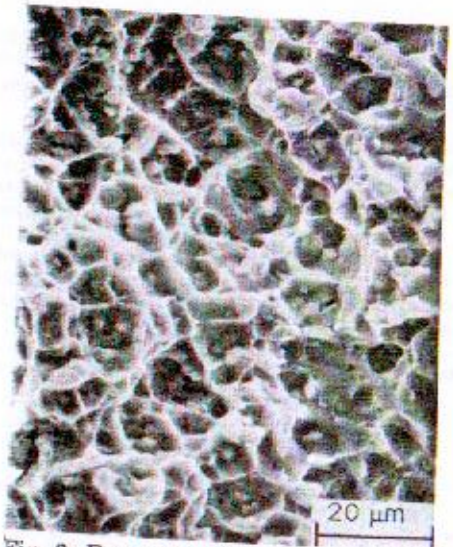

Fig. 2. Fracture surface of 2618 Al alloy.

Fig. 3a. Fracture surface of 2618 Al alloy + 15% SiC (T4).

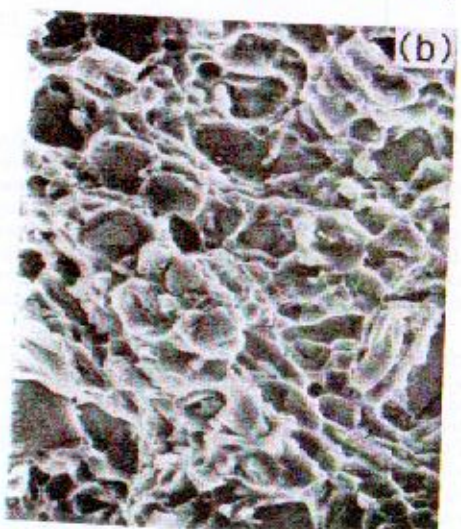

Fig. 3b. Fracture surface of 2618 Al + 15% SiC (T651).

Fig. 3c. Detail of SiC particulates on the fracture surface (T651).

an average diameter over 5 μm (marked with A in Fig. 4) and smaller ones with large aspect ratio and oriented in the extrusion direction (marked with B in Fig. 4). It is not clear whether all these particulates were broken during the tensile tests or prior to testing, as a result of the thermo-mechanical treatments. However, these results are in

agreement with the drop in the composite elastic properties during deformation and with the presence of broken particulates in the fractured surfaces, which suggests that particulate fracture is the mechanism responsible of the reduced ductility of this spray formed MMC.

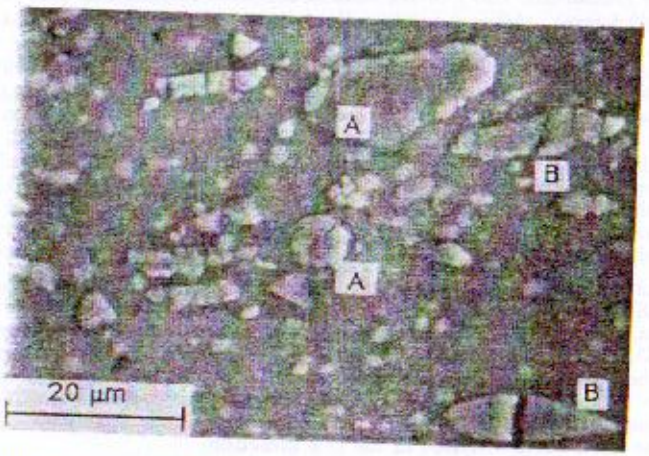

Fig. 4. Broken SiC particulates. Loading axis is horizontal.

DISCUSSION

The differences in ductility between the composites in T4 and T651 conditions arise because particulate fracture takes place earlier during deformation in the latter, as is shown by the faster reduction in modulus and the larger number of broken particulates found on the fracture surfaces. The actual number of particulates broken during deformation is difficult to assess because it is likely that a significant number cracked when the material was extruded and stretched. However, an estimation can be obtained from the work of Mochida *et al.* (1991), who used a combination of Eshelby's equivalent inclusion method and Mori-Tanaka's back stress analysis, to study the effect of cracked particulates on the stiffness of a MMC. Eshelby's method illustrates the modification of the elastic properties of a homogeneouos solid due to an ellipsoidal inclusion. With Mori-Tanaka's back stress analysis, the interaction between two types of inhomogeneities (particulates and cracked particulates), and that between an inhomogeneity and the outer boundary, is accounted for. So the results are valid even for large volume fractions of reinforcement. SiC particulates are considered as spheres, with elastic properties given by E_p=450 GPa and ν_p=0.17 (LLorca *et al.*, 1991). Broken particulates are modelled as penny-shaped cracks, the crack plane perpendicular to the loading axis. The matrix elastic properties were E_m=70 GPa and ν_m=0.33. The relation between the composite Young's modulus, E_c, and the matrix modulus is given by

$$\frac{E_c}{E_m} = \frac{1}{1 + \eta_1(1-r)f + \eta_2 fr} \qquad (1)$$

where f is the volume fraction of particulates, r the fraction of broken particulates, and η_1 and η_2 are coefficients which can be found in Mochida (1991). The volumen fraction of broken particulates, r, can be estimated from (1) as a function of the applied strain, and the results are plotted in Fig. 5. It is clear that particulate fracture develops very quickly in the T651 condition and almost one third of the particulates are cracked for

an applied strain of about 0.03, leading to specimen failure. On the contrary, only 7% of the particulates have been broken in the underaged composite at the same strain, and r reaches 20% only after extensive plastic deformation. It is worth noting that these values are upper limits because other factors, such as extensive cavitation in the matrix, can contribute to the degradation of the Young's modulus, especially for strains very close to the fracture strain.

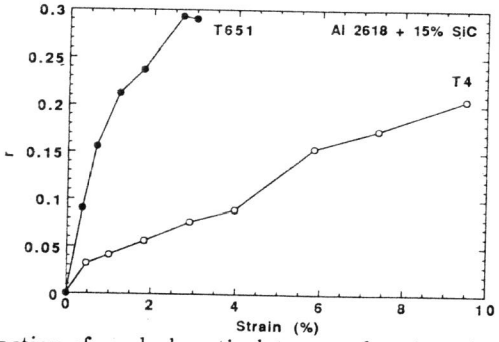

Fig. 5. Volume fraction of cracked particulates as a function of the applied strain.

The limiting effect of particulate fracture in MMC's ductility under monotonic (LLoyd, 1991) and cyclic loads (LLorca *et al.*, 1992) has already been reported, but the role of matrix strength on the volume fraction of broken particulates is not clear. Lloyd (1991) found more cracked particulates on the fracture surfaces of peak-aged 6061 Al-based composite reinforced with 10 and 20 vol. % SiC than on those of the underaged material. With aging time there was an increase in the composites yield strength with aging time, associated with a reduction in ductility. He also pointed out, however, that particulate fracture extends throughout the gauge length in the T4 temper and it is very localized around the fracture surface in the T6, with a larger number of broken particulates in the former.

A finite element study was performed to ascertain the evolution of stresses and strains in the matrix and in the reinforcement during deformation, and therefore the causes of particulate fracture. The composite is modelled as a periodic array of identical cells. Each cell has a particulate in the center, embedded within the matrix. Axisymmetric cylindrical cells, which can be regarded as an approximation to a three dimensional array of hexagonal cylinders, are used in the calculations (LLorca *et al.*, 1991). Due to the symmetry, only one fourth of the cell has to be analysed and the particulate shape is cylindrical with equal height and diameter. Consideration is restricted to deformations for which straight lines bounding each cell remain straight after deformation (this is a stronger constraint imposed by periodicity). Further detailsof the boundary conditions can be found in LLorca *et al.* (1991). The particulates are considered to remain elastic during deformation, whereas the Al matrix behaves as an elastic-plastic material, with isotropic hardening and Von Mises flow rule. Matrix properties for each temper were obtained from the tensile tests of the unreinforced alloy.

The results of the analyses are shown in Figs. 6 to 7. Contour plots of plastic strain in the matrix for T4 and T651 tempers are presented in Figs. 6a and 6b respectively, when the far-field strain is close to the fracture strain in each material. The presence of the ceramic reinforcement gives rise to a localization of the strains in the matrix around the particulates, even for small far-field strains. This strain localization is clearly observed in Figs. 3a and 3b. As matrix deformation increases, the constraint imposed by the surrounding cells leads to the development of large tensile hydrostatic stresses in the matrix. The joint effect of strain localization (which produces void initiation around the intermetallic inclusions by inclusion fracture or debonding) and triaxiality (which

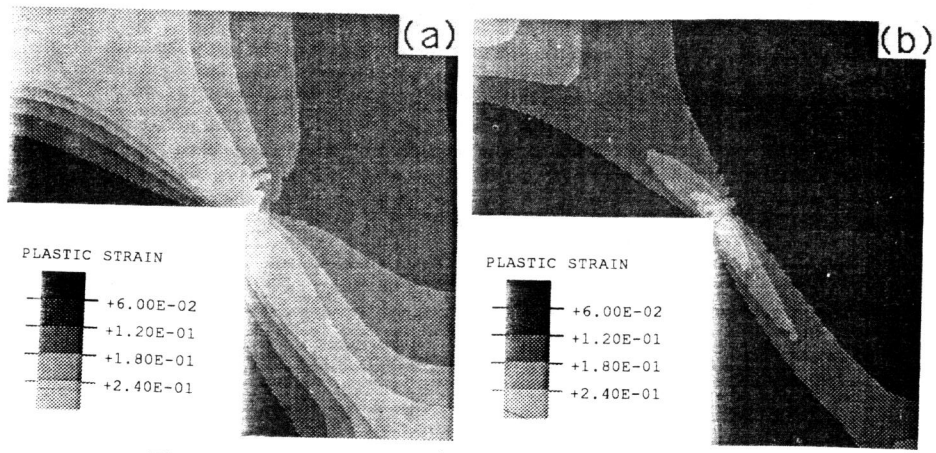

Fig. 6. Contour plots of plastic deformation in the matrix. (a) T4, ϵ= 0.12 (b) T651, ϵ= 0.04.

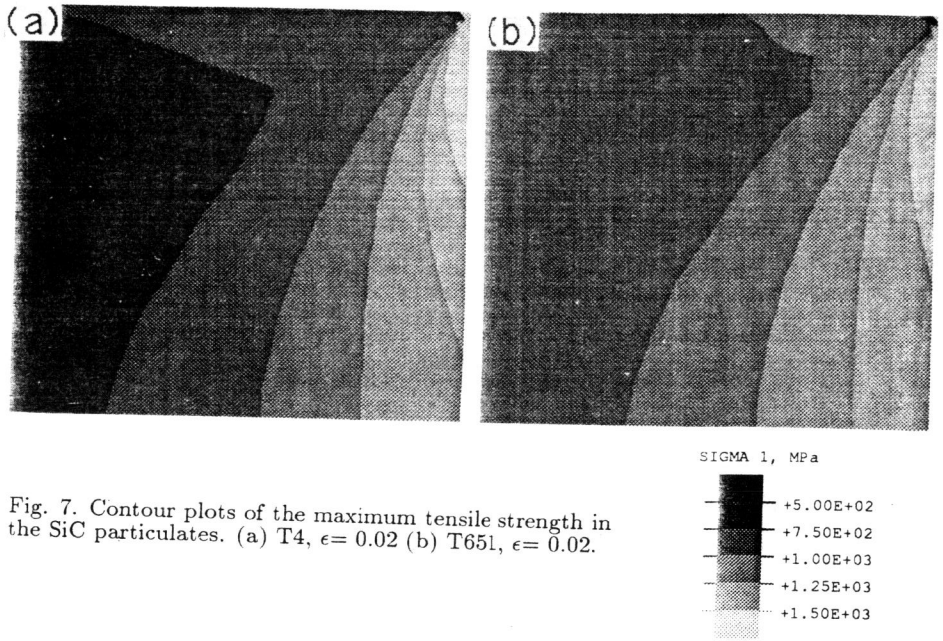

Fig. 7. Contour plots of the maximum tensile strength in the SiC particulates. (a) T4, ϵ= 0.02 (b) T651, ϵ= 0.02.

accelerates void growth rate) can produce the failure of the composite by the mechanism of void coalescence. This phenomenon was analysed in detail by LLorca *et al.*(1991)

who showed that the ductility in the peak-aged condition is only slightly lower than that of the underaged material when the composite is reinforced with particulates, and the volume fraction, size and shape of inclusions remain constant. Hence this mechanism cannot be responsible for a two fold reduction in ductility, as shown in Table 1.

The contour plots of the maximum principal stress in the SiC particulates are shown in Fig. 7a and 7b for T4 and T651 conditions respectively, when the far-field strain is 0.02. The tensile stresses in the particulates in the peak-aged composite are far larger than in the underaged, and therefore more particulates are expected to crack in the former condition. The fracture of ceramic particulates is statistical and is controlled by the size of the flaws in the particulates. Large particulates, which are more likely to have larger defects, are prone to break more easily than smaller ones under the same stress. In addition, particulates with high aspect ratio, oriented in the loading direction carry more load than equiaxed ones and will be subjected to higher tensile stresses. Our observations (see Fig. 4) are in agreement with these considerations.

The finite element analyses show that the volume fraction of cracked particulates should increase with the matrix strength when other failure mechanisms, such as matrix cavitation or interfacial debonding, are restrained. However, it is important that this result is obtained on the basis of a homogeneous distribution of the particulates. This assumption is valid for spray formed MMCs, where the solidification process is very fast and the particulates are evenly distributed at microscopic level within the matrix. However, cast MMCs exhibit a high degree of particulate clustering and particulate fracture tends to increase in these zones, regardless of the matrix properties.

Despite the relatively low ductility of the spray formed composite in the T651 condition, its fracture toughness is surprisingly good, as compared with other MMCs of similar strength. This is mainly a consequence of the manufacturing process, which leads to clean strong interfaces and to a homogeneous distribution of the particulates. Particulate clusters are regions of preferential damage accumulation ahead of blunt notches or propagating fatigue cracks (Lewandowski *et al.*, 1989) and they lower substantially the resistance to crack initiation. Another favorable factor is the large average size of the particulates. The fractographic analysis indicates that fracture in the T651 temper is controlled by cracked particulates which act as voids in front of the crack tip. On the contrary, the growth of voids formed around the intermetallic inclusions is inhibited because triaxial stresses are relieved when the particulates crack. The linkage of the voids formed around the broken particulates requires the presence of large plastic strains over a distance equal to the interparticulate spacing. Thus, for a given volume fraction of reinforcement, the energy dissipated by plastic deformation around the crack tip increases with the particulate size. The experimental results of Kamat *et al.* (1989) agree with this model for 2XXX Al alloys reinforced with 2 to 20% vol. Al_2O_3 particulates with an average particulate size between 5 and 15 μm. However, more detailed investigations are required to reach definitive conclusions on the effect of particulate size and shape on fracture toughness.

CONCLUSIONS

The deformation and failure mechanisms in a spray formed 2618 Al alloy reinforced with SiC particulates were studied. The stiffness and the tensile properties of the composite show a significant improvement whereas the fracture toughness is the same as that of unreinforced alloy. The only drawback is the marked reduction in tensile ductility in the peak-aged condition. Experimental and numerical analyses indicated that coarse SiC particulates are broken very early during composite deformation, leading to the formation of voids which finally coalesce. This process is more acute in the peak-aged condition because the higher the matrix strength, the higher the stresses in the particulates. Thus a reduction in the average particulate size (by sieving the largest ones) would increase the tensile ductility of this material. The excellent fracture toughness of the composite is related to several factors, including the homogeneous distribution of the reinforcement, the interfacial strength, and the large size of the particulates. Large particulates lead to large interparticulate spacing, which improves the capacity of energy dissipation by plastic deformation in front of the crack tip prior to fracture. The reduction in particulate size to enhance the tensile ductility should be accompanied by other actions to maintain the fracture properties. The use of cleaner matrices, without Fe and Ni, seems a reasonable choice.

Acknowledgements

This work has been supported by the EEC, through contract BREU-075C, and by CICYT, Spain, under grant MAT92-32.

REFERENCES

Arsenault, R. J., Shi, N., Feng, C. R., and Wang, L. (1991) Localized Deformation of SiC-Al Composites, *Materials Science and Engineering*, A131, pp. 55-68.

Goolsby, R. D. and Austin, K. L. (1989) Fracture Toughness of Discontinuous SiC Reinforced Al Alloys. In: *Advances in Fracture Research, ICF7*, (Salama, K. *et al.*, Eds.), pp. 2423-2435, Pergamon, New York.

Healy, J. C. and Beevers, C. J. (1991) A Study of Fatigue Crack Growth in a Particulate-Reinforced Al-Si alloy at 23 and 220°C, *Materials Science and Engineering*, A142, pp. 183-192.

Mochida, T., Taya, M. and Obata, M. (1991) Effect of Damaged Particles on the Stiffness of a Particle-Metal Matrix Composite, *JSME International Journal*, 34, pp. 187-193.

Nakagawa, A. H. and Gungor, M. N. (1990) Microstructure and Tensile Properties of Al_2O_3 Particle Reinforced 6061 Al Cast Composite. In: *Fundamental Relationships Between Microstructure and Mechanical Properties of Metal-Matrix Composites*, (Liaw, P. K. and Gungor, M. N., Eds.), pp. 127-143, TMS, Warrendale, PA.

Kamat, S. V., Hirth, J. P., and Mehrabian, R. (1989) Mechanical Properties of Particulate-Reinforced Aluminum-Matrix Composites, *Acta Metallurgica*, 37, pp. 2395-2402.

Lewandowski, J. J., Liu, C. and Hunt, W. H. (1989) Effects of Matrix Microstructure and Particle Distribution on Fracture of an Aluminum Matrix Composite, *Materials Science and Engineering*, A107, pp. 241-255.

LLorca, J., Needleman, A. and Suresh, S. (1991) An Analysis of the Effects of Matrix Void Growth in Deformation and Ductility in Metal-Ceramics Composites, *Acta Metallurgica et Materialia*, 39, pp. 2317-2335.

LLorca, J., Suresh, S. and Needleman, A. (1992) An Experimental and Numerical Study of Cyclic Deformation in Metal-Matrix Composites, *Metallurgical Transactions*, 23, pp. 919-934.

Lloyd, D. J. (1991) Aspects of Fracture in Particulate-Reinforced Metal-Matrix Composites, *Acta Metallurgica et Materialia*, 39, pp. 59-71.

McDanels, D. L. (1985) Analysis of Stress-Strain, Fracture and Ductility Behavior of Aluminum Matrix Composites Containing Discontinuous Silicon Carbide Reinforcement, *Metallurgical Transactions*, 16A, pp. 1105-1115.

Roebuck, B. and Lord, J. D. (1990) Plane Strain Fracture Toughness Test Procedures for Particulate Metal Matrix Composites, *Materials Science and Technology*, 6, pp. 1199-1209.

Suresh, S., Christman, T. and Sugimura, Y. (1989) Accelerated Ageing in Cast Al Alloy-SiC Particulate Composites, *Scripta Metallurgica*, 23, pp. 1599-1602.

Willis, T. C. (1988) Spray Deposition Process for Metal Matrix Composites Manufacture, *Metals and Materials*, 4, pp. 485-488.

Zhang, D. L. and Cantor, B. (1991) Private communication.